AL-AZHAR ENGINEERING SIXTH
INTERNATIONAL CONFERENCE
1 - 4 SEPTEMBER 2000

AEIC 2000

مؤتمر الأزهر الهندسي الدولي
السادس
١ - ٤ سبتمبر ٢٠٠٠م

AN EXPERIMENTAL STUDY OF FORCED CONVECTION IN HORIZONTAL POROUS ANNULI

E. F. Atwan; A. R. El-Shamy and K.M. El-Shazly
Mech. Eng. Dept. Faculty of Eng. (Shoubra), Zagazig Univ.,
108 Shoubra St., Cairo, Egypt, Fax 202-2023336.

ABSTRACT
This paper investigates experimentally the flow and heat transfer characteristics in horizontal annuli filled with porous media. With air as the working fluid, the effects of the annulus radius ratio, flow velocity and particle thermal conductivity are examined for a wide range of thermal conductivity (from 61 W/m K for carbon steel to 0.16 W/m K for polyvinyl chloride), radius ratio (inner/outer) ranging from 0.200 to 0.625 and a range of Reynolds number from 5200 to 12000. The results indicate that, in the presence of particles, the measured average Nusselt number was up to four times higher than that for an annulus without spherical particles. It was found that higher heat transfer coefficients are obtained with packing particles of higher thermal conductivity. Also, the average Nusselt number always increases as the radius ratio increases. The present experimental data are compared against those available in the literature and good correspondence is noticed. Furthermore, an empirical correlation for the average Nusselt number with the governing dimensionless parameters was developed.

KEYWORDS
Forced convection; heat transfer; porous media; horizontal annulus.

INTRODUCTION
Forced convection heat transfer through porous media has been the subject of intensive studies in recent years, because of its important engineering applications such as thermal insulation engineering, water movement in geothermal reservoirs, underground spreading of chemical waste, nuclear waste repository, grain and coal storage, solid matrix heat exchangers, enhanced recovery of petroleum reservoirs, drying technology, and many others. This increased use of porous media has made it essential to have a better understanding of the associated transport processes.

The majority of the previous investigations include the flow through packed beds of spheres and packed cylinders. Most of these studies dealing the problem of forced convection with numerical or analytical models. For theoretical simulation of the transport phenomena in porous media, Vafai and Tien (1981) used a non-Darcian model to account for the boundary and inertia effects in forced convection. Vafai et al. (1985), Beckerman and Viskanta (1987), Cheng and Zhu (1987), and Renken and Poulikakos (1987, 1988) studied the forced convection in the porous media with effects of flow inertia, thermal dispersion,

variable porosity, and Brinkman friction. All the above-mentioned theoretical studies adopted the local thermal equilibrium assumption for formulating the energy equation.
Koh and colony (1974) and Koh and Stevens (1975) studied the forced convection in a porous channel filled with a high conductivity porous material by using the Darcy flow model. They reported that the wall temperature and the wall-to-coolant temperature difference decrease drastically in the channel with a constant heat flux. In a numerical investigation based on Brinkman-extended flow model, Kaviany (1985) reported results for forced convection in a porous channel bounded by isothermal parallel plates. Ergun (1952), Kuo and Nydegger (1978), and Jones and Krier (1983) investigated the flow drag through porous channel with porosity from 0.38 to 0.65. Rowe and Claxton (1965) measured the heat transfer performance in porous channels. Cheng et al. (1988) analyzed the forced convection in the entrance region of a packed channel with asymmetric heating. Vafai and Sozen (1990) presented an analysis of the forced gas flow through a packed bed of spherical particles. They used the fluid-to-solid heat transfer coefficients from an empirical correlation established by Gamson et al. (1943). The results showed that the local thermal equilibrium condition was very sensitive to the particle Reynolds number and the Darcy number. Amiri and Vafai (1994) simulate numerically the forced convective incompressible flow through porous media and the associated transport processes. Kamuto and Saitoh (1994) examined numerically the fully developed forced convection heat transfer in cylindrical packed beds with constant wall temperatures based on a two-dimensional model incorporating the effects of non-Darcy, variable porosity and radial thermal dispersion. Hwang et al. (1994, 1995) found that the value of the heat transfer coefficient between the solid and the fluid phases might affect seriously the estimation of the heat transfer performance in a high conductivity porous channel. The structure and porosity of the porous media may also affect the flow patterns and thermal transport phenomena in the porous channels. Adnani et al. (1995) examined numerically convective heat transfer in a particle packed tube. Axial and radial dispersion are both included in the governing equations. They reported that the heat transfer in the thermally developing region is affected by axial dispersion when Peclet number is smaller than 10. Khalil et al. (2000) presented a numerical investigation of forced convection heat transfer through a packed pipe with constant heat flux. The effects of particle Reynolds number, pipe-to-particle diameter ratios and Prandtl number are presented.
Very few studies on forced convection through a porous medium are experimental. Among these experimental studies, the work reported by Vafai et al. (1985). Their investigation focused on porous media flat plate boundary layer forced convection for a matrix consisting of 5 and 8-mm-diameter packed spheres. Comparisons of experimental and numerical results were presented for the average Nusselt number as a function of the Reynolds number based on pore diameter and the two types of beads used. Renken and Poulikakos (1989) presented an experimental investigation of boundary-layer forced convective heat transfer from a flat isothermal plate in a packed bed of spheres. Extensive experimental results are reported for the thermal boundary-layer thickness, the temperature field, and the local wall heat flux (represented by the local Nusselt number). Chen and Yue (1991) studied theoretically and experimentally the thermal performance of packed capsules in an ice water storage system for air conditioning. Nasr et al. (1994) investigated experimentally forced convection heat transfer from a cylinder embedded in a packed bed of spherical particles. Wu and Hwang (1998) studied experimentally and theoretically the flow and heat transfer characteristics inside packed and fluidized beds. Their results show that the heat transfer coefficient increases with the decrease of the porosity and the increase of the particle Reynolds number. El Kady (2000) simulated experimentally forced convection heat transfer

from a circular pipe exposed to constant heat flux and filled with porous media of particle to pipe diameter ratios d/D>0.5.

A few studies have been reported on forced convection in an annular cavity. Wang and Du (1993) analyzed experimentally the forced convective heat transfer in a vertical annulus filled with porous media. Al-Nimr et al. (1994) solved numerically the problem of transient laminar forced convection in the entrance region of a porous concentric annulus considering both Darcian and non-Darcian effects on the flow. El Kady (1994) investigated numerically the forced convection heat transfer and flow in an annular channel filled with porous media taking into consideration the non-darcian effects (flow inertia, variable porosity and Brinkman friction). Using the Darcy-Brinkman model, analytical solutions were obtained by Chikh et al. (1995a) for the problem of forced convection in an annular duct partially filled with a porous medium. The same problem was investigated numerically by the same group (1995b) using the Darcy-Brinkman-Forchheimer model. Recently, Al-Nimr and Alkam (1997) presented numerical solutions for forced convection in concentric annuli partially filled with porous substrates. The porous substrate is attached either to the inner cylinder (case I), or to the outer cylinder (case O). They reported that porous substrates might improve Nusselt number by 1200 percent keeping other flow and geometrical parameters fixed.

The above mentioned investigations consider forced convection problems in different composite geometries. Most of these studies are based on numerical or analytical solutions. The experimental results are still few. However, to the best of the authors' knowledge, there have not been any investigations on forced convection through horizontal annular porous cavities taking into consideration the curvature effect in the open literature. The objective of this work is to present an experimental investigation for forced convection in a horizontal annular porous layer exposed to a uniform heat flux from the outside circular tube. Attention is focused on the effect of curvature (radius ratio) on heat transfer rate (represented by the average Nusselt number). In addition, the study is extended to show the effect of particle thermal conductivity where three packing materials are tested for a wide range of particle thermal conductivity.

EXPERIMENTAL APPARATUS AND PROCEDURES

The experimental apparatus employed in this investigation is shown schematically in Fig. 1(a). It consists of a blower assembly, test-section, porous medium, and instrumentation to measure temperatures, pressure drop, air flow rate, and electrical power input. The details of the apparatus are depicted as follows:

(a)Air Blower: A centrifugal type air blower of 150 mm inlet section diameter, 600 mm outer blade diameter and 105x105 mm square outlet section, driven by an A.C. motor of 3 hp capacity and 3000 rpm normal speed, is used to supply the system with air at the required flow rate. The airflow rate can be controlled via the blower intake gate.

(b)Test Section: A longitudinal section of the packed annulus is illustrated in Fig.1(b). The test section is a horizontal annular passage formed by two concentric tubes. The outer one is a circular brass tube of 40-mm inner diameter, 3.5-mm thickness. The inner tube is alumina with outer diameters of 8, 12, 18, 25 mm to give a wide range of the radius ratio. Heat is only transferred from the inner surface of the outer tube while the inner tube is filled with an insulating material. The test section has 3-m length, representing a length-to-diameter ratio of about 75 and an additional 3-m hydrodynamic entry length is allowed upstream of the test section inlet. The test section is connected to the entrance tube through a flexible connection and it is heated by means of an electric heater made from a nickel-chromium wire while a guard heater is used to prevent heat loss. The entire heated test

section is insulated with a high temperature insulating asbestos rope, which is 13-mm diameter wound around the main heater and provides high thermal resistance.

(c) Porous Medium: The porous media used in the experiments were packed beds of solid spheres with a nominal diameter 6-mm . This nominal diameter corresponds to 6.35 mm for carbon steel, 5.65 mm for sand grains, and 6.25 mm for Polyvinyl Chloride (PVC). The thermal conductivity of the three tested materials is 61, 1.83, and 0.16 W/mK, respectively. The sand "spheres" are, in fact, not exactly spherical but have a narrow size distribution for which the equivalent diameter is determined from the lower and upper limits of the DIN standard sieving analysis (5.00/6.30). The porosity was estimated separately by measuring the volume of water that needed to fill the void space for a known volume of particles. It will be considered ε=0.380 as a mean value of the measured porosity for the three different particle sizes. The packing material was carefully placed into the test section to ensure uniformity in the structure of the porous matrix. The same packing was used in all experiments. The spheres are held in place at both ends of the test section by rigid meshed screens.

(d) Instrumentation: The wall temperatures were measured at several axial positions (40 different test positions with higher concentration at tube inlet) using thermocouples made of copper-constantan wires of 0.5 mm diameter, and connected to a multi channel digital thermometer of accuracy 0.1°C. At each axial location, at least two diametrically opposed top-bottom, thermocouples are fixed on the tube wall to check the axisymmetry of the flow. Details of the test section cross-section with the wall thermocouples fixation at a selected test position are shown in Fig.1(c). The airflow radial temperature profile is measured via radiation shielded thermocouples mounted on vertical traverse mechanisms at tube inlet and exit, respectively. The thermocouple probe with its radiation shield is made with small sizes compared with the annular flue gap. To avoid flow disturbance, the thermocouple probe with its shield are resided in a tubular-cavity which is externally assembled normal to the test annulus such that the probe appears only in the flow field at the instant of reading.

Also, the flow rate was measured by a calibrated orifice-meter connected to an inclined micromanometer, having five different scales with a minimum division of 10 Pa, via two taps. A system of U-tube manometers is used for measuring the axial pressure distribution along the test section. The power is supplied via a voltage regulator to control the heat flux input to the test section. An ammeter and a logging multimeter are used to measure current and voltage, respectively.

The steady state was assumed to be established if the wall temperature and air flow temperatures changed within 0.2 °C during 15 minutes. Then the data of electric power input, the temperaure distribution on the heating surface, inlet and exit air flow temperatures, and manometers readings were recorded.

METHOD OF CALCULATIONS

All the individual temperature measurements are first corrected using their corresponding calibration curves as well as the air flow rate. The annular test section is divided into 16 axial segments with unequal lengths (highly concentrated at the entrance). The temperature readings are averaged to give an average surface temperature for each segment and for the entire test section. The power input to the heaters was computed from measurements of the voltage and current and then the average heat flux to the test section was obtained. The heat lost by axial conduction, radial conduction through the insulation layers and by radiation from the two ends of the test section are very small and can be neglected for the tested range of parameters. Also, the average heat flux to the test section was obtained by measurement of the average increase in bulk temperature of flowing air across the test

section. The average increase in bulk temperature may be found by measuring the bulk temperatures at the entrance and exit of the test section. Since the values of the mass flow rate and the specific heat of air are known quantities, the heat flux may be calculated. This measurement was used just as a check of the heat flux measurement by the power input to the electrical heater. The heat balance was found to be less than 5%.

Knowledge of the average heat flux q" and the surface average temperatures of the test annulus segments allowed for the computation of the local heat transfer coefficient h_x from the defining equation:

$$h_x = \frac{q''}{\overline{T}_{w,x} - \overline{T}_{f,x}} \tag{1}$$

where,

- q" is the heat flux ($Q_{heater}/\pi DL$)
- $T_{w,x}$ is the local surface mean temperature of the test annulus segment
- $T_{f,x}$ is the local flow mean temperature at the annular segment, calculated from the heat balance for each segment as follows:

$$mC_p(T_{f,x}-T_{f,x-\Delta x})=q''(\pi D\Delta x) \tag{2}$$

Thus, the flow outlet temperature at the streamwise station x is:

$$T_{f,x}=T_{f,x-\Delta x}+q''(\pi D\Delta x)/\, mC_p \tag{3}$$

where, Δx is the annular segment length. Therefore, the flow mean temperature for each segment was calculated as the arithmetic mean between the inlet and outlet as:

$$\overline{T}_{f,x} = \left(T_{f,x} + T_{f,x-\Delta x}\right)/2 \tag{4}$$

The local Nusselt number based on the annulus outer diameter (D_o) is evaluated as:

$$Nu_x = \frac{h_x D_o}{k_f} = \frac{q'' D_o}{k_f\left(\overline{T}_{w,x} - \overline{T}_{f,x}\right)} \tag{5}$$

and the average Nusselt number is the calculated by simply integrating the local values as:

$$\overline{Nu} = \frac{1}{L}\int_0^L Nu_x dx \tag{6}$$

The average Nusselt number, based on the annulus outer diameter (D_o), may be simply calculated as:

$$\overline{Nu} = \frac{\overline{h}\, D_o}{k_f} = \frac{q'' D_o}{k_f\left(\overline{T}_w - \overline{T}_b\right)} \tag{7}$$

where T_w is the average wall temperature of the heated outer tube, T_b is the bulk bed-air temperature, and k_f is the fluid thermal conductivity.

Also, the flow Reynolds number based on the annulus outer diameter (D_o) is given by the defining equation:

$$\mathrm{Re}_{D_o} = \frac{UD_o}{\nu} \tag{8}$$

where U is the airflow mean velocity at test section inlet (approaching velocity).
The Fanning friction factor F_f in terms of the flow frictional pressure drop along the annular porous test section is given by:

$$F_f = \left(\frac{\Delta P}{2\rho U^2} \right) \frac{D_o}{L} \tag{9}$$

The thermophysical air properties (e.g. density, specific heat, viscosity, and thermal conductivity) were based on the film temperature and calculated using regression curve fits (ASHRAE, 1976).
An uncertainty analysis was performed for evaluation of the accuracy of the experimental measurements. The percentage of uncertainty in the measurement of V, R, A, T_s, and T_f are 1.0, 0.6, 0.5, 1.0, and 1.0, respectively. Thus the uncertainty in the heat transfer coefficient was estimated to be ±4.1 percent..

RESULTS AND DISCUSSION

Experiments were carried out to investigate the effect of Reynolds number, packing material thermal conductivity, and the annulus radius (diameter) ratio on the heat transfer rate and pressure drop along horizontal porous annuli heated from the outer wall. Three packing materials of nominal particle size 6 mm having thermal conductivities 0.16 W/mK for Polyvinyl Chloride (PVC) spheres, 1.83 W/mK for sand particles, and 61 W/mK for carbon steel spheres were tested for annulus radius (diameter) ratios of 0.20, 0.30, 0.45, and 0.625 within a range of Reynolds number from 5200 to 12000.
A total of 60 experimental runs were carried out for the flow through packed annuli with different radius ratios for the three tested packing materials. The variations of the local Nusselt number along the test section for the Polyvinyl Chloride spheres, sand particles, and carbon steel spheres at different annulus radius ratios for various Reynolds numbers are presented in Figs.(2a-c). From the figures it can be seen that the local Nusselt number is high along the thermal entry region and reaches the asymptotic value in the fully-developed region. Also, the higher the Reynolds number, the longer the thermal entrance length. When (x/D)>30, the thermal boundary can be considered as fully-developed. The local Nusselt number for the thermally-developed region changes with Re, and hence is quite different from that for the laminar flow through empty annuli, for which Nu depends only upon the wall thermal conditions. This is due to the lateral mixing of the fluid due to 'turbulence' caused by successive flow disturbance through packed beds, i.e. the significant effect of thermal dispersion on the thermal boundary layer developed and therefore on the heat transfer coefficient (Wang and Du 1993). It was also noticed from figs.2(a)-(c) that the higher values for the local Nusselt numbers are for steel particles at high radius ratio, η=0.625.
To illustrate the effectiveness of the particles in enhancing the heat transfer rate, a comparison of sample results for the bare (smooth) annulus (η=0.300) to one filled with 6 mm nominal diameter PVC, sand, and steel particles is presented in Table 2. The ratio of the Nusselt number for the packed annulus to that for a bare annulus is presented in the last

Table 2 Heat transfer enhancement due to the presence of porous matrix inside the annulus (η=0.300)

Re_D	Packed annulus Particle Material	Nu, packed	Bare annulus, Nu, Bare	Ratio
5212	PVC	25.34	11.53	2.19
12050	PVC	55.41	22.32	2.48
5200	Sand	30.25	11.40	2.65
11942	Sand	63.36	22.20	2.85
5273	Steel	38.83	12.01	3.23
12100	Steel	93.33	22.78	4.09

column of the table. It is observed that the packed annulus increases the average Nusselt number greatly (up to four times for carbon steel spheres), indicating that the particles serve as effective enhancers for forced convection heat transfer. The heat transfer augmentation produced by the porous matrix is attributed to a combination of effects, including thinning the hydrodynamic and thermal boundary layers around the outer heated wall of the annulus, increased mixing (thermal dispersion), and direct conduction through the porous matrix.

The effect of particle conductivity on heat transfer rate, represented by the average Nusselt number, is illustrated in Figs.3(a)-(d). The average Nusselt number is plotted versus Reynolds number for the three tested materials namely PVC, sand, and carbon steel at various annulus radius ratios within the range of Reynolds number from 5200 to 12000. The figures show that the average Nusselt number increases with the increase of particle conductivity and the highest average Nusselt number is associated with the use of carbon steel as the packing material. This increase is attributed to the high thermal conductivity of the carbon steel, which results in high contact conduction to particles touching the outer heated wall of the annulus. Thus, it is concluded that for a constant particle size, an increase in particle conductivity yields an increase in the heat transfer rate in terms of the average Nusselt number.

Figures 4, 5, and 6 show the variation of the average Nusselt number with Reynolds number and radius ratio for annuli filled with the three tested packing materials, PVC, sand, and steel, repectively. It is noticed from the figures that an increase in Reynolds number yields an increase in the average Nusselt number for all radius ratios and all packing materials. Also, it can be seen that the average Nusselt number increases with increasing the radius ratio η for the same packing material. This result is noticed for all the three tested packing materials. For the same inlet flow rate to the test section (nearly the same Reynolds number), increasing the radius ratio η (i.e. decreasing the annulus gap width, D_o-D_i) leads to faster flow and giving rise to thinner velocity boundary layers and consequently higher heat transfer rates in terms of the average Nusselt number. It must be noted that in figs. (3-6) the Nusselt numer values for smooth tubes, evaluated from the well-established Dittus-Boelter correlation listed in Incropera and DeWitt (1985), are also plotted for reference.

Based upon the experimental heat transfer results, a general correlation that accounts for the governing parameters was developed by expressing the average Nusselt number as a function of the governing dimensionless groups as:

$$\overline{Nu} = a\,Re^{b}(k_s/k_f)^{c}\,\eta^{d} \qquad (10)$$

where a, b, c, and d are empirical constants obtained from least-squares fitting of the expermental data. The appearance of the Reynolds number in the correlation is accounts for the flow average inlet velocity U, while the dimensionless ratios (k_s/k_f) and (η=r_i/r_o) are

used to account for the different particle thermal conductivities and the effect of the annulus radius ratio, respectively. Using a least-squares approach, the values of the constants a, b, c, and d are 0.033, 0.785, 0.079, and 0.267, respectively. Therefore, the general form of the empirical correlation for the present experimental heat transfer results is:

$$\overline{Nu} = 0.033\,\mathrm{Re}^{0.785}\,(k_s / k_f)^{0.079}\,\eta^{0.267} \qquad (11)$$

This correlation is valid for the following range of parameters:

$$5200 \le \mathrm{Re} \le 12000\,,\quad 6.45 \le k_s/k_f \le 2300\,,\ 0.200 \le \eta \le 0.625$$

where the Nusselt and Reynolds numbers are based on the annulus outer diameter and the fluid thermal conductivity. The predictions of Eq.(11) are compared to the measured values of average Nusselt numbers in Fig. 7 for all packing materials at all various radius ratios. It may be seen that of the 60 data points plotted on the figure, 94 percent lie within ±14% of the correlating equation.

Finally, Figs. 8 and 9 are sample graphs illustrating the total pressure drop and friction factor, respectively, through the packed annulus for different radius ratios within the tested range of Reynolds number. Figure 8 illustrates that the total pressure drop across the acked annulus increases with the increase of Reynolds number. Also, for a fixed value of Reynolds number, which is based on the mean inlet velocity, the pressure drop increases with the increase of the annulus radius ratio (decrease of annulus gap width). This increase is attributed to the increased velocity with decreasing the annular gap width, which results in a decrease in pressure (i.e. increasing the pressure drop across the annulus). The Fanning friction factors evaluated from Eq. (9) are plotted against the Reynolds numbers for different radius ratios in Fig. 9. The predictions of Kuo and Nydegger (1978) for friction factor through porous channel is presented on the same graph. The correlation of Techo et al. (1965) for turbulent flow in smooth tubes is:

$$F_s = 4\left[1.7372\ln\left(\frac{\mathrm{Re}}{1.964\ln\mathrm{Re} - 3.8215}\right)\right]^{-2} \qquad (12\backslash$$

Kakac et al. (1987) suggested the following multiplier for the Techo et al. correlation, which would enable prediction of smooth-annulus friction factors in the range $5000<\mathrm{Re}<10^7$

$$F_{s,a} = F_{s,t}\,(1+0.0925\eta) \qquad (13$$

where the subscript s,a refers to a smooth annulus, and the subscript s,t refers to a smooth tube. The modified correlation is also plotted in Fig. 9 for two radius ratios, η=0.200 and 0.625, for reference. It can be seen from the graph that the friction factor depends on the Reynolds number. The difference between the measured values of friction factors and values obtained from the literature is due to different geometries of the test sections.

CONCLUSIONS

This paper presented an experimental investigation for the problem of forced convection through horizontal packed annuli. The main focus of this research is to study the effect of the annulus radius ratio on heat transfer rates, which has typically ignored by most investigators. The study is extended to show the effect of the particle conductivity, where three packing materials having a wide range of thermal conductivity $6.45 \le k_s/k_f \le 2300$ were tested. The following conclusions are drawn from the data presented:

1- The presence of particles in an annulus enhances the heat transfer greatly when compared to the case of a bare (smooth) annulus (up to four times for carbon steel spheres), indicating that the particles serves as effective enhancers for forced convection heat transfer.

2- The thermal entrance length depends on the Reynolds number. The higher the Reynolds number, the longer the thermal entry length. When (x/D)>30, the thermal boundary can be considered as fully-developed.
3- The average Nusselt number increases with the increase of particle conductivity and the highest value is associated with the use of carbon steel spheres as the packing material.
4- For the same packing material and the same radius ratio, the average Nusselt number increases with increasing the Reynolds number.
5- The radius ratio η is an important parameter in forced convection through packed annuli. The average Nusselt number increases with increasing the annulus radius ratio for the same packing material.
6- The total pressure drop across the packed annulus increases with the increase of Reynolds number and/or the radius ratio η. Also, the friction factor depends only on Reynolds number.
7- New single correlation for the present experimental heat transfer results was developed utilizing least-squares curve fitting of the form:

$$\overline{Nu} = 0.033\,\mathrm{Re}^{0.785}\,(k_s / k_f)^{0.079}\,\eta^{0.267}$$

which is valid for $5200 \leq Re \leq 12000$, $6.45 \leq k_s/kf \leq 2300$, and $0.200 \leq \eta \leq 0.625$.

REFERENCES

Adnani P., Catton I., and Abdou M. A. (1995), Non-Darcian Forced Convection in Porous Media With Anisotropic Dispersion, ASME Journal of Heat Transfer, Vol. 117, pp. 447-451.

Al-Nimr M. A. and Alkam M. K.(1997), Unsteady Non-Darcian Forced Convection Analysis in an Annulus Partially Filled With a Porous Material, ASME Journal of Heat Transfer, Vol. 119, pp. 799-804.

Al-Nimr M. A., Aldoss T. K. and Naji M. I. (1994), Transient Forced-Convection in the Entrance Region of Porous Concentric Annuli, Candian Journal of Chemical Engineering, Vol. 72, No. 6, pp. 1092-1096.

Amiri A. and vafai K. (1994), Analysis of Dispersion Effects and Non-Thermal Equilibrium, Non-Darcian, Variable Porosity Incompressible Flow Through Porous Media, Int. J. Heat Mass Transfer, Vol. 37, No. 6, pp. 939-954.

ASHRAE (1976), Thermophysical Properties of Refrigerants, New York.

Beckerman C. and Viskanta R. (1987), Forced Convection Boundary Layer Flow and Heat Transfer Along a Flat Plate Embedded in a Porous Medium, Int. J. Heat Mass Transfer, Vol. 30, No. 7, pp. 1547-1551.

Chen S. L. and Yue J. S. (1991), Water Thermal Storage with Solidification, Heat Recovery System & CHP, Vol. 8, pp. 247-254.

Cheng P. and Zhu H. (1987), Effects of Radial Thermal Dispersion on Fully Developed Forced Convection in Cylindrical Packed Bed, Int. J. Heat Mass Transfer, Vol. 30, No. 7, pp. 2373-2383.

Cheng P., Hsu C.T. and Chowdhury A. (1988), Forced Convection in the Entrance Region of a Packed Channel With Asymmetric heating, ASME Journal of Heat Transfer, Vol. 110, pp. 946-954.

Chikh S., Boumedien A., and Lauriat G. (1995a), Analytical Solution of Non-Darcian forced Convection in an Annular Duct Partially Filled with a Porous Medium, Int. J. Heat Mass Transfer, Vol. 38, pp. 1543-1551.

Chikh S., Boumedien A., and Lauriat G. (1995b), Non-Darcian forced Convection Analysis in an Annular Partially Filled with a Porous Material, Numerical Heat Transfer Part A, Vol. 28, pp. 707-722.

El Kady M. (1994), Forced Convection Heat Transfer and Flow in an Annular Porous Medium in the Non-Darcian Effects, Mansoura Engineering Journal (MEJ), Vol. 19, No. 3, pp. M9-M-26.

El Kady M. (2000), Enhancement of Forced Convection Heat Transfer From a Cylindrical Pipe Using Porous Media of High Diameter Ratios, 11th Int. Mechanical power Engineering Conference, Cairo, Vol. 1, pp. H159-H173.

Ergun S. (1952), Fluid Flow Through Packed Columns, Chemical Engineering Progress, Vol. 48, pp. 89-94.

Gamson B. W., Thodos G., and Hougen O. A. (1943), Heat, Mass and Momentum Transfer in Flow of Gases, Trans. AIChE, Vol. 39, pp. 1-35.

Hwang G. J. and Chao C. H. (1994), Heat Transfer Measurement and Analysis for Sintered Porous Channels, ASME Journal of Heat Transfer, Vol. 116, pp. 456-464.

Hwang G. J., Wu C. C., and Chao C. H. (1995), Investigation of Non-Darcian Forced Convection in an Asymmetrically Heated Sintered Porous Channel, ASME Journal of Heat Transfer, Vol. 117, pp. 725-732.

Incropera F. P. and DeWitt D. P. (1985), Fundamentals of Heat and Mass Transfer, 2nd ed., John Wiley and Sons, New York.

Jones D. P. and Krier H. (1983), Gas Flow Resistance Measurements Through Packed Beds at High Reynolds Numbers, ASME Journal of Fluids Engineering, Vol. 105, pp. 168-173.

Kakac S., Shah R. K., and Aung W. (1987), Handbook of Single-Phase Convective Heat Transfer, Wiley, New York.

Kamiuto K. and Saitoh S. (1994), Fully Developed Forced-Convection Heat Transfer in Cylindrical Packed Beds With Constant Wall Temperatures, JSME International Journal, Series B. Vol. 37, No. 3, pp. 554-559.

Kaviany M. (1985), Laminar Flow Through a Porous Channel Bounded by Isothermal Parallel Plates, Int. J. Heat and Mass Transfer, Vol. 28, pp. 851-858.

Khalil R. A., El-Shazly K. M. and Assasa G. R. (2000), Heat Transfer and Fluid Flow Characteristics of Forced Convection Through a Packed Pipe, 11th Int. Mechanical power Engineering Conference, Cairo, Vol. 1, pp. H186-H200.

Koh J. C. Y. and Colony R. (1974), Analysis of Cooling Effectiveness for Porous Material in Coolant Passages, ASME Journal of Heat Transfer, Vol. 96, pp. 324-330.

Koh J. C. Y. and Stevens R. L. (1975), Enhancement of Cooling Effectiveness by Porous Materials in Coolant Passage, ASME Journal of Heat Transfer, Vol. 97, pp. 309-310.

Kuo K. K. and Nydegger C. C. (1978), Flow Resistance Measurements and Correlation in a Packed Bed of WC 870 Ball Propellants, Journal of Ballistics, Vol. 2, No. 1, pp. 1-25.

Nasr K., Ramadhyani S. and Viskanta R. (1994), An Experimental Investigation on Forced Convection Heat Transfer From a Cylinder Embedded in a Packed Bed, ASME Journal of Heat Transfer, Vol. 116, pp. 73-80.

Renken K. J. and Poulikakos D. (1987), Forced Convection in Channel Filled with Porous Medium, Including the Effects of Flow Inertia, Variable Porosity, and Brinkman Friction, ASME Journal of Heat Transfer, Vol. 109, pp. 880-888.

Renken K. J. and Poulikakos D. (1988), Experiment and Analysis of Forced Convection Heat Transfer in a Packed Bed of Spheres, Int. J. Heat Mass Transfer, Vol. 31, pp. 1399-1408.

Renken K. J. and Poulikakos D. (1989), Experiments on Forced Convection From a Horizontal Heated Plate in a Packed Bed of Glass Spheres, ASME Journal of Heat Transfer, Vol. 111, pp. 59-65.
Rowe P. N. and Claxton K. T. (1965), Heat and Mass Transfer From a Single Sphere to Fluid Flowing Through an Array, Trans. Instn. Chem. Engrs., Vol. 43, pp. T321-T331.
Techo R., Tickner R. R., and James R. E. (1965), An Accurate Equation for the Computation of the Friction Factor for Smooth Pipes From the Reynolds Number, J. Appl. Mech., Vol. 32, p. 443.
Vafai K. and Tien C. L. (1981), Boundary and Inertia Effects on Flow and Heat Transfer in Porous Media, Int. J. Heat Mass Transfer, Vol. 24, pp. 195-203.
Vafai K., Alkire R. I. and Tien C. L. (1985), An Experimental Investigation of Heat Transfer in Variable Porosity Media, ASME Journal of Heat Transfer, Vol. 107, pp. 642-647.
Vafai K. and Sozen M. (1990), Analysis of the non-thermal equilibrium Condensing Flow of a Gas through a Packed Bed, Int. J. Heat Mass Transfer, Vol. 33, No. 6, pp. 1247-1261.
Wang B. and Du J. (1993), Forced Convective Heat Transfer in a Vertical Annulus Filled With Porous Media, Int. J. Heat Mass Transfer, Vol. 36, No. 17, pp. 4207-4213.
Wu C. C. and Hwang G. J. (1998), Flow and Heat Transfer Characteristics Inside Packed and Fluidized Beds, ASME Journal of Heat Transfer, Vol. 120, pp. 667-673.

NOMENCLATURE

SI system of units was applied for the whole parameters used in this paper.

A	surface area
C_p	working fluid (air) specific heat
D	outer diameter of the outer tube
D_i	inner diameter of the annulus
D_o	outer diameter of the annulus
d_p	nominal diameter of the particles
h	heat transfer coefficient
k_f	thermal conductivity of air
k_s	thermal conductivity of spheres
L	annular tube length
m	air mass flow rate
p	pressure
q''	heat flux
R	electric heater resistance
T	temperature
U	mean axial flow velocity
V	voltage
x	axial distance measured from annulus inlet

Greek letters:

Δ	difference
ε	porosity
ν	kinematic viscosity of the fluid
μ	dynamic viscosity of the fluid
ρ	density
η	radius (diameter) ratio

Subscripts:

D	based on annulus outer diameter
in	at annulus inlet
f	for fluid
o	case of smooth annulus flow
out	at annulus exit
w	at wall
x	local value

Superscripts:

—	average value.

Dimensionless Terms:

F_f	Friction factor
Nu	Nusselt number
Pr	Prandtl number
Re	Reynolds number

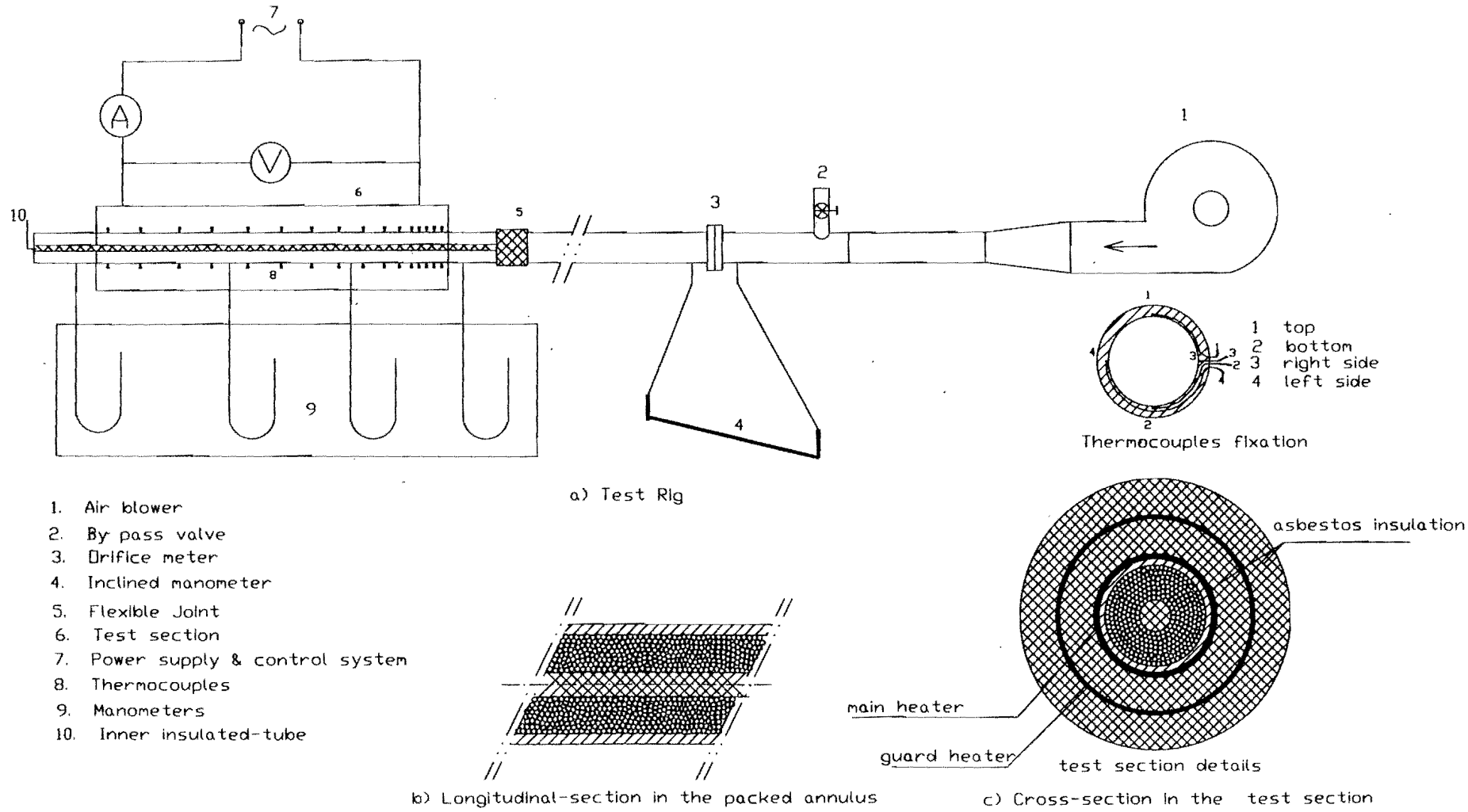

Fig. 1 Schematic diagram of the experimental Setup

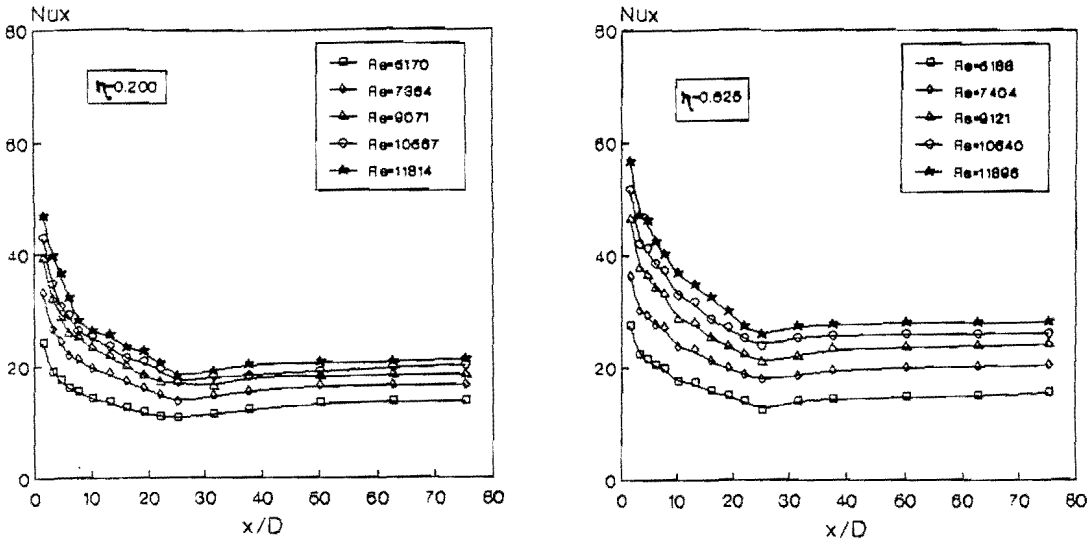

(a) PVC spheres

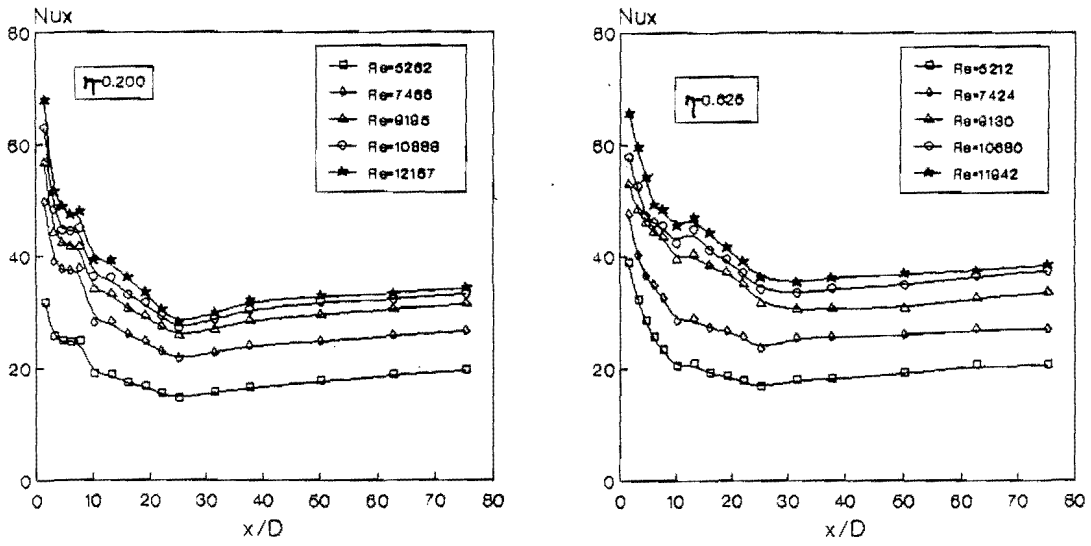

(b) Sand Particles

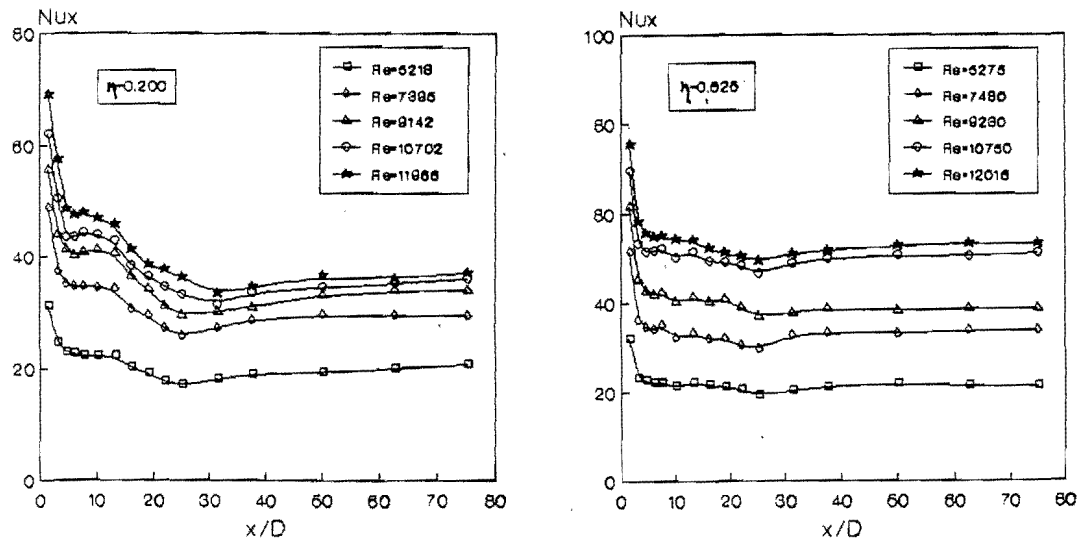

(c) Steel spheres

Fig.2 Variation of local Nusselt number with x/D at different Reynolds numbers for various packing materials, (a) PVC spheres; (b) Sand particles; and (c) Carbon steel spheres.

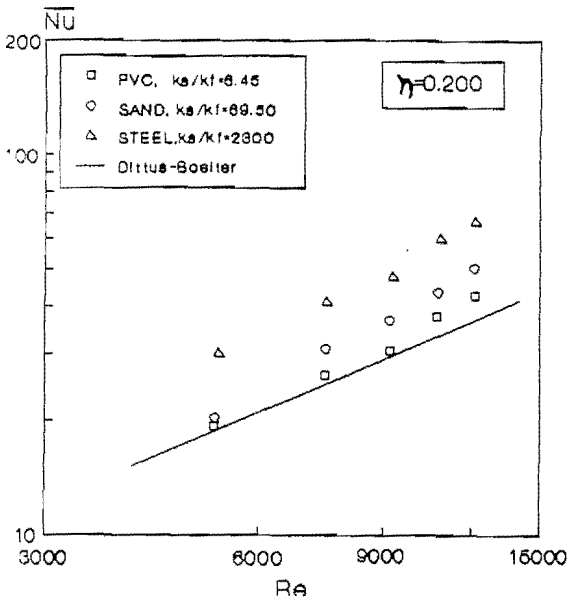

(a) η=0.20

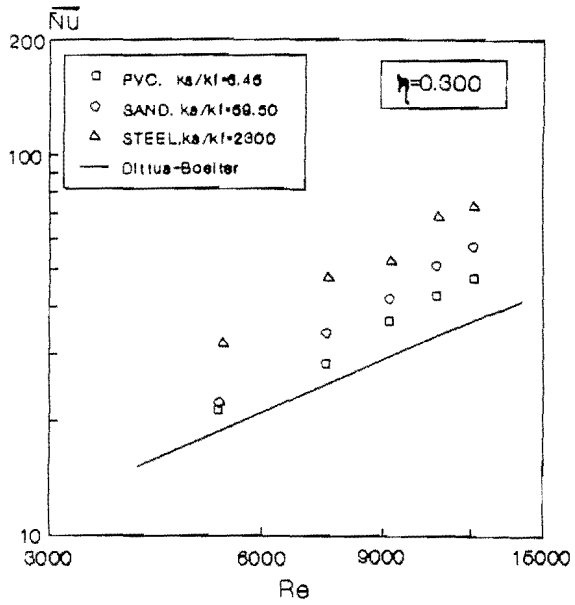

(b) η=0.30

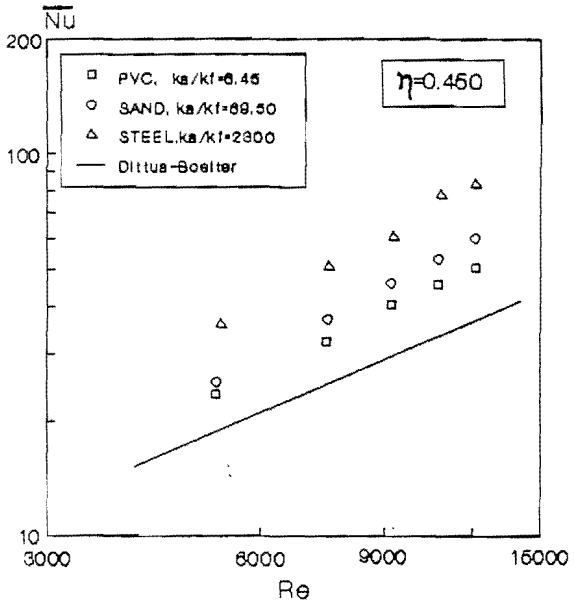

(c) η=0.45

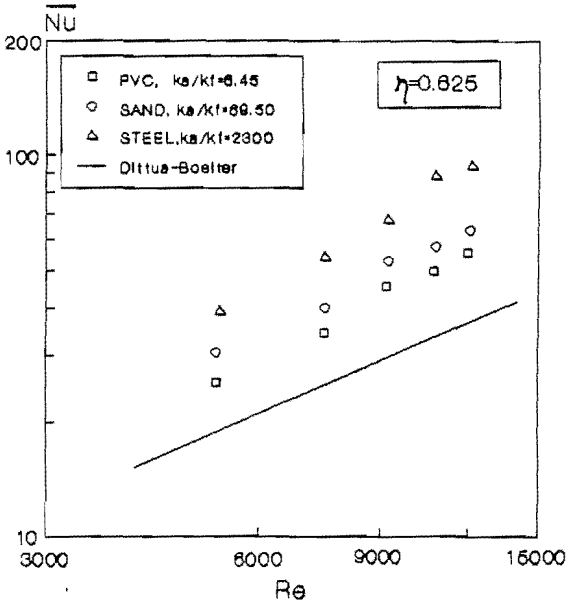

(d) η=0.625

Fig. 3 Effect of particle conductivity on the average Nusselt numbers at different radius ratios, (a) η=0.20; (b) η=0.30; (c) η=0.45; (d) η=0.625.

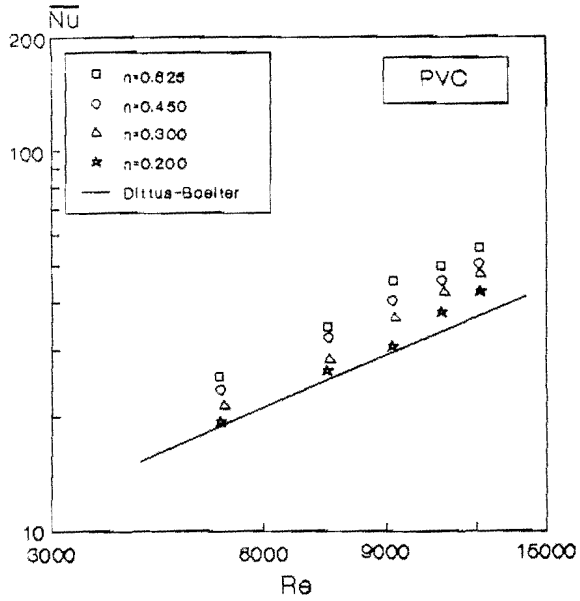

Fig. 4 Variation of average Nusselt number with Reynolds number and radius ratio for annuli filled with PVC spheres.

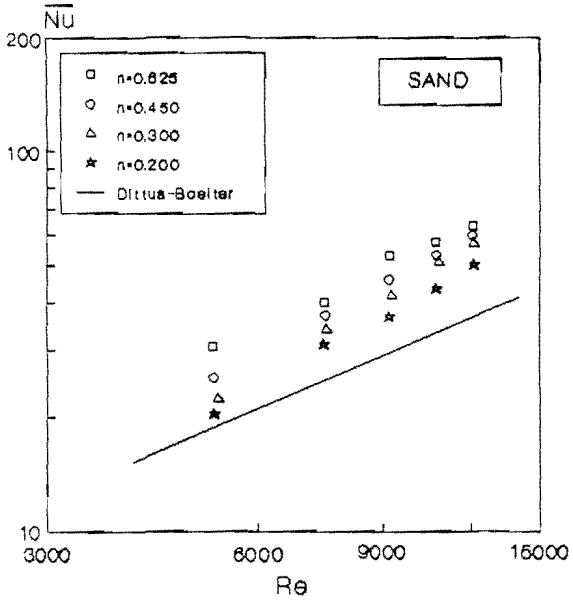

Fig. 5 Variation of average Nusselt number with Reynolds number and radius ratio for annuli filled with sand particles.

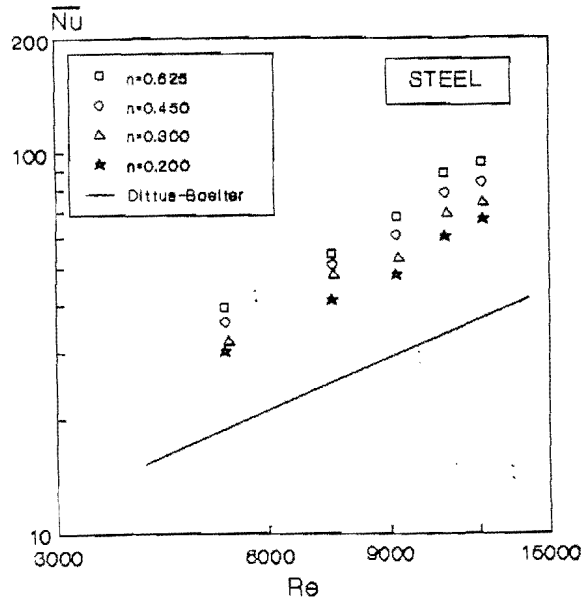

Fig. 6 Variation of average Nusselt number with Reynolds number and radius ratio for annuli filled with steel spheres.

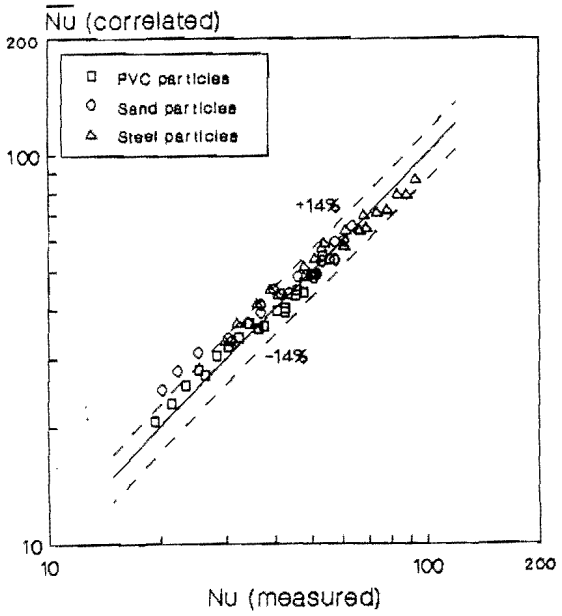

Fig. 7 Comparison of measured Nusselt numbers with those obtained from present correlation.

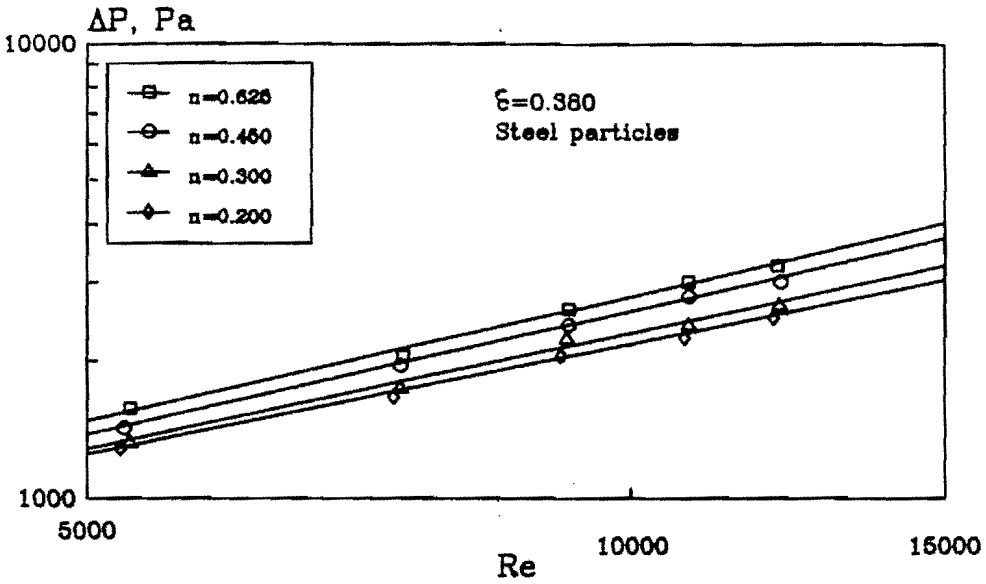

Fig. 8 Pressure drop through the packed annulus at different radius ratios.

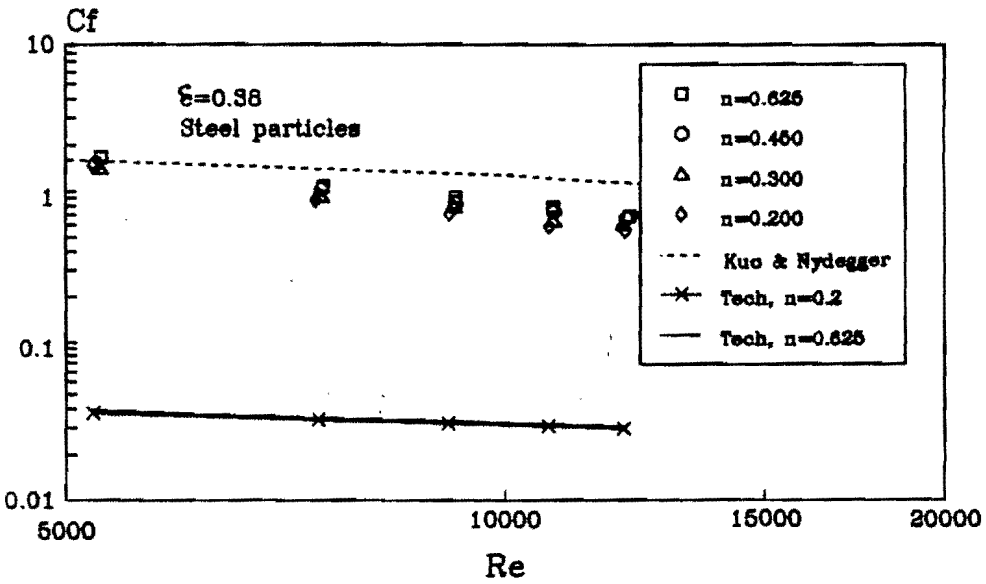

Fig. 9 Friction factor versus Reynolds number at different radius ratios for packed annuli with steel particles.